tvst

Cornea & External Disease

Design and Biocompatibility of a Novel, Flexible Artificial Cornea

Gavin Li[1,2], Anthony J. Aldave[3], Guillermo Amescua[4], Kathryn A. Colby[5], Maria S. Cortina[6], Jose de la Cruz[6], Jean-Marie A. Parel[4], Thomas B. Schmiedel[7], and Esen Karamursel Akpek[1]

[1] The Ocular Surface Disease Clinic, The Wilmer Eye Institute, Johns Hopkins University School of Medicine, Baltimore, MD, USA
[2] Icahn School of Medicine at Mount Sinai, New York, NY, USA
[3] Stein Eye Institute, David Geffen School of Medicine at UCLA, Los Angeles, CA, USA
[4] Bascom Palmer Eye Institute, University of Miami-Miller School of Medicine, Miami, FL, USA
[5] Department of Ophthalmology at New York University Grossman School of Medicine, New York University, NY, USA
[6] Illinois Eye and Ear Infirmary, University of Illinois, Chicago, IL, USA
[7] Innovation Center of Excellence, W. L. Gore & Associates, Inc., Newark, DE, USA

Correspondence: Esen Karamursel Akpek, The Ocular Surface Disease Clinic, The Wilmer Eye Institute, Johns Hopkins University School of Medicine, 1800 Orleans Street, Woods 372, Baltimore, MD 21287-9238, USA. e-mail: esakpek@jhmi.edu

Received: December 20, 2023
Accepted: April 16, 2024
Published: May 22, 2024

Keywords: corneal transplantation; keratoprosthesis; biocompatibility

Citation: Li G, Aldave AJ, Amescua G, Colby KA, Cortina MS, de la Cruz J, Parel JMA, Schmiedel TB, Akpek EK. Design and biocompatibility of a novel, flexible artificial cornea. Transl Vis Sci Technol. 2024;13(5):19, https://doi.org/10.1167/tvst.13.5.19

Purpose: We sought to introduce the materials, design, and biocompatibility of a flexible and suturable artificial corneal device.

Methods: Single-piece, fully synthetic, optic-skirt design devices were made from compact perfluoroalkoxy alkane. The skirt and the optic wall surfaces were lined with a porous tissue ingrowth material using expanded polytetrafluoroethylene. Full-thickness macroapertures around the skirt perimeter were placed to facilitate nutrition of the recipient cornea. Material properties including the skirt's modulus of elasticity and bending stiffness, optic light transmission, wetting behavior, topical drug penetrance, and degradation profile were evaluated.

Results: The final prototype suitable for human use has a transparent optic with a diameter of 4.60 mm anteriorly, 4.28 mm posteriorly, and a skirt outer diameter of 6.8 mm. The biomechanical and optical properties of the device closely align with the native human cornea with an average normalized device skirt-bending stiffness of 4.7 kPa·mm^4 and light transmission in the visible spectrum ranging between 92% and 96%. No optical damage was seen in the 36 devices tested in fouling experiments. No significant difference was observed in topical drug penetrance into the anterior chamber of the device implanted eye compared with the naïve rabbit eye.

Conclusions: The flexibility and biocompatibility of our artificial cornea device may offer enhanced tissue integration and decreased inflammation, leading to improved retention compared with rigid keratoprosthesis designs.

Translational Relevance: We have developed a fully synthetic, flexible, suturable, optic-skirt design prototype artificial cornea that is ready to be tested in early human feasibility studies.

Introduction

Corneal disease represents the fourth leading cause of preventable vision loss globally.[1] An estimated 6.17 million individuals live with bilateral corneal blindness (defined by the World Health Organization as visual acuity of worse than 3/60).[1–3] A particularly unfortunate aspect is that, unlike other eye diseases that predominantly affect older individuals, corneal blindness disproportionately affects a younger population. In India, 15.8% of all blindness and moderate-to-severe visual impairment is owing to corneal disease, with 44% of corneal blindness occurring in patients younger than 50 years, with the most common etiology being childhood keratitis (36.7%).[1,2] Fortunately, vision can be

restored in the majority of the cases through donor corneal transplantation.[3] However, despite being the most widely performed form of tissue or organ transplantation globally, there is a significant scarcity of donor corneas, with only 1 in 70 individuals who would benefit from donor corneal transplantation having access to the surgery.[3,4] In addition, not all patients who undergo donor corneal transplantation will have vision improvement. Graft failure is not uncommon in patients with other comorbidities such as aphakia or corneal neovascularization, as well as in pediatric patients or patients with glaucoma or after glaucoma surgery.[5] It is well-known that the outcome of corneal transplantation is largely determined by the preoperative indication for surgery.

The landscape of corneal transplantation has changed dramatically in the last two decades with the introduction of endothelial keratoplasty for Fuchs' dystrophy and collagen cross-linking for keratoconus. These developments led to a significant decrease in the number of individuals with these two most favorable preoperative indications undergoing penetrating keratoplasty (PK). From 2000 to 2021, the proportion of PKs performed in the United States decreased from 98.8% of all grafts to 33.1%.[6,7] Previous graft failure is now the leading indication for PK in North America, as well as Europe.[7–10] It is well-known that both graft survival and visual outcomes worsen with each successive surgery.[11] Therefore, the outcomes of today's PK surgeries are likely not as favorable as those that historically reported graft clarity rates of up to 93% at 25 years after surgery.[12]

Currently, keratoprosthesis, or artificial corneal transplantation, is considered in eyes with a limited expectation of success from donor corneal transplantation, such as those with repeated previous failures. The most commonly implanted prosthetic corneal device globally is the Boston type I keratoprosthesis (Massachusetts Eye and Ear Infirmary, Boston, MA). Although the device yields superior outcomes compared with repeat PK in many patients,[13–15] the annual number of implantations has trended downward, with the latest studies reporting on worsening outcomes with longer term follow-up.[16–20] Owing to the limitations of current artificial corneas, currently there is no device that is suitable as a replacement for donor corneal transplantation to address the global donor shortage.[21,22]

We herein created a single-piece, fully synthetic corneal device with optic and skirt configuration that is flexible and suturable. The surgery is a single step, minimally invasive, and does not require a fresh donor cornea. The surgical technique and short-term clinical and histopathological outcomes in a rabbit model have been published.[23,24] Here, we report the developmental considerations and biomechanical properties of the newer version designed for human use to be tested in early feasibility clinical studies.

Methods

Human Device Design

The human device design has been modified from the rabbit prototype.[23] The device dimensions as well as refractive power have been adjusted for human cornea. It is a single-piece, optic-skirt design made of a proprietary (W. L. Gore & Associates, Inc., Newark, DE) flexible, suturable, optically clear fluoropolymer, perfluoroalkoxy alkane that comprises the device core. The human device exhibits a 4.60-mm optic diameter anteriorly and a 4.28-mm diameter posteriorly, with an optic stem thickness of 1.20 mm and an outer skirt diameter of 6.9 mm (Fig. 1). These dimensions were established after several reiterations to ensure excellent apposition between the recipient cornea and the optic stem at the completion of the surgery which is essential for biointegration. Multiple experiments were performed testing post-mortem adult human globes with varying degrees of corneal swelling using the commercially available 4-mm disposable hand-held metal trephines for surgery. The ratio between the trephination diameter (3.0 mm) vs. the optical stem diameter (3.35 mm) proven to work well for Boston type I keratoprosthesis implantation was factored into the mathematical equations. Optical coherence tomography images after implantation were performed to ensure optimal fit. The optical stem curvature and thickness were adjusted according to average human corneal curvatures to provide final refractive power suitable for pseudophakic human eye. The anterior and posterior surfaces of the skirt and the optic wall are lined with porous expanded polytetrafluoroethylene for

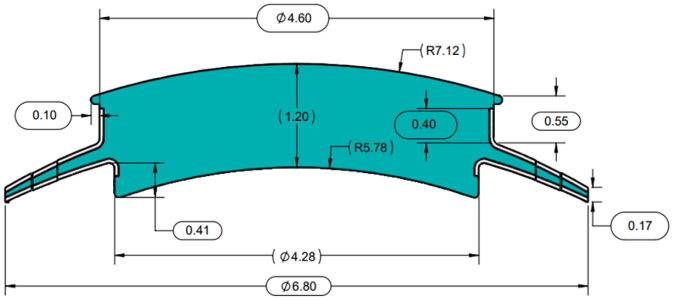

Figure 1. Diagram of the revised device being prepared for human implantation (all original dimensions are in millimeters, drawn to scale).

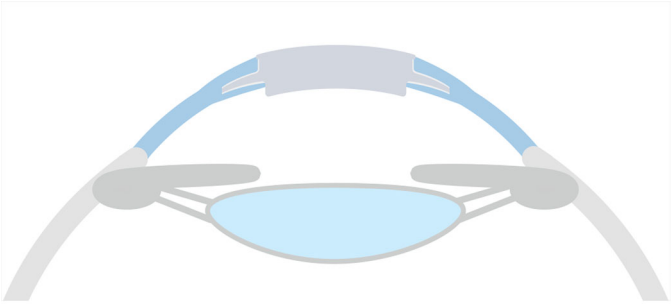

Figure 2. Diagram demonstrating the device (gray) implanted within the recipient corneal stroma (blue).

integration into the recipient cornea at the device tissue joint. The optic surface does not support epithelial growth.

The expanded polytetrafluoroethylene layer is bonded in a manner to minimize the risk of separation and peeling, which have not been observed. The ingrowth surfaces are rendered hydrophilic and become translucent when moist. The device is implanted within an intrastromal pocket in the recipient cornea with the optic exposed to the ocular surface anteriorly and anterior chamber posteriorly (Fig. 2). The device is secured within the stromal pocket with 16 permanent sutures placed through the skirt. Sixteen circumferential macroapertures placed along the skirt allow for nutrient and hydration flow to the anterior lamella from the aqueous humor to prevent desiccation and necrosis of the cornea anterior to the skirt.

The optic diameter of the human device measures 4.60 mm with a central thickness of 1.2 mm, whereas the anatomically shaped tapered skirt measures 6.8 mm in its outer diameter with an approximately average thickness of 0.2 mm. The optic is shaped to yield the desired refractive power of 43.5 diopters while approximating the natural curvature of the human eye, resulting in an outer radius of curvature of 7.1 mm and an inner radius of curvature of 5.8 mm, appropriate for implantation in a pseudophakic human eye.

Elasticity and Stiffness

Young's modulus is a measure of elasticity, which is the ratio of the stress acting on a substance to the strain (deformation) produced:

$$Youngs\ modulus\ (E) = \frac{Uniaxial\ stress\ force\ per\ unit\ surface}{Strain} = \frac{\sigma}{\varepsilon}.$$

Young's modulus for the human cornea, which varies according to age, was sourced from three previous reports,[25–27] and an average value was derived for reference.

The bending stiffness is the resistance of an item against bending deformation. It is linearly dependent on Young's modulus and geometric factors. In the case of a flat sheet, the bending stiffness is proportional to the thickness cubed as well as the width of the sheet. The bending stiffness of the device can be calculated, taking into consideration the thickness of the skirt, Young's modulus of the core material, and an equivalent width of 1 mm. To obtain Young's modulus, we performed a complex modulus measurement on an ARES-G2 rheometer (TA Instruments, New Castle, DE). We measured the material viscoelastic properties across a temperature range using an oscillation temperature ramp on an 8-mm parallel plate geometry. Using the measured complex modulus and Poisson's ratio of the viscoelastic core material (0.5), we obtained Young's modulus of the fluoroelastomer at 30°C, which represents an upper bound of Young's modulus as the material slightly softens with temperature. For reference, the temperature on the ocular surface is 32.8°C to 35.5°C, depending on when it is measured during the blink cycle.[28]

$$\text{Bending stiffness} = \mathrm{E} * \mathrm{I}$$

with E being Young's modulus and I being the cross-sectional moment of inertia for a thin plate:

$$I = \frac{1}{12} * w * t^3$$

where w is the width of the plate and t is the thickness of the plate. The bending stiffness calculation was performed for the skirt of the device at its thickest section at the optic-skirt junction (240 microns) and at its thinnest section at the skirt edge (170 microns) using a plate width of 1 mm.

Light Transmission Through the Optic

Transmission spectra of the core material were measured in air using a Shimadzu-UV-2600 spectrometer (Shimadzu Corp., Kyoto, Japan), fitted with an integrating sphere and reported as a total transmission spectrum between 250 and 900 nm wavelengths. The baseline reference spectrum was measured without the device being present and was recorded as 100%.

Fouling and Wettability of the Optic

Fouling refers to the deposition of mineral salts and/or biologic matter on the surface or within the body of a transparent synthetic polymer device that is in direct contact with tissues.[29] A list of topical

Table. Results of Spoliation of the Device Optic With Commonly Used Diagnostic and Therapeutic Topical Medications

Pharmaceutical Tested	Drug Class	Optic Stem	Optic Surface
Saline	Control	3/3 clear	3/3 clear
Latanoprost 0.005%	Glaucoma	3/3 clear	2/3 clear 1/3 with local white deposit
Timolol maleate 0.5%	Glaucoma	3/3 clear	3/3 clear
Moxifloxacin 0.3%	Antibiotic	3/3 clear	3/3 clear
Polymyxin B/trimethoprim[a]	Antibiotic	3/3 clear	3/3 clear
Tobramycin/dexamethasone[b]	Antibiotic	3/3 clear	3/3 clear
Vancomycin 25 mg/mL	Antibiotic	3/3 clear	3/3 clear
Prednisolone acetate 1%	Steroid	6/6 clear	4/6 clear 2/6 white nonuniform deposits
Cyclosporine 0.5%	Anti-inflammatory	3/3 clear	3/3 clear
Fluorescein sodium/benoxinate[c]	Diagnostic	3/3 clear	3/3 clear
Phenylephrine HCl 2.5%	Diagnostic	3/3 clear	3/3 clear

[a]Polymyxin B sulfate 10,000 U/mL; trimethoprim sulfate equivalent to 1 mg/mL.
[b]Tobramycin 0.3%; dexamethasone 0.1%.
[c]Fluorescein sodium 0.25%; benoxinate 0.4%.

drugs commonly used in the field of ophthalmology for diagnosis or treatment of a condition was created for investigation (Table).

Individual synthetic cornea devices were first placed into a vial containing approximately 0.5 mL of each commercially available pharmaceutical to immerse the device in its entirety. The vial was then incubated for 24 hours at 37°C while on an orbital shaker set at 180 cycles/min. After 24 hours, the devices were removed and placed in a vial containing approximately 0.5 mL of artificial aqueous humor (Biochemazone, Alberta, Canada) and then incubated again for 24 hours at 37°C on an orbital shaker set at 180 cycles/min. Devices were not rinsed during the change. Exposure to 0.9% saline followed by artificial aqueous humor was used as a control.

The devices were then placed in vials of deionized water for storage. Devices were removed from deionized water, lightly patted dry with a nonshedding cloth, and observed via light microscopy for any defects. Images of the post-exposure devices were created at magnifications ranging from 25× to 200×. Three devices were tested per topical medication.

The wetting behavior of the devices was assessed during the rabbit surgical experiments[26] while in situ at monthly intervals up to 12 months under an operating microscope. Fluorescein drops (fluorescein sodium/benoxinate hydrochloride 0.25%/0.4%; Altaire Pharmaceuticals Inc., Aquebogue, NY) were instilled directly onto the device after having placed a wire lid speculum. The eye was inspected under the operating microscope with a low magnification and a broad beam using a cobalt blue filter to visualize the entire device optic and the device tissue joint. The fluorescein stains the preoptic tear film and appears green in color (Fig. 3). The appearance of a black spot indicates the break-up in the predevice tear film. Tear film break-up time is the time interval between the instillation

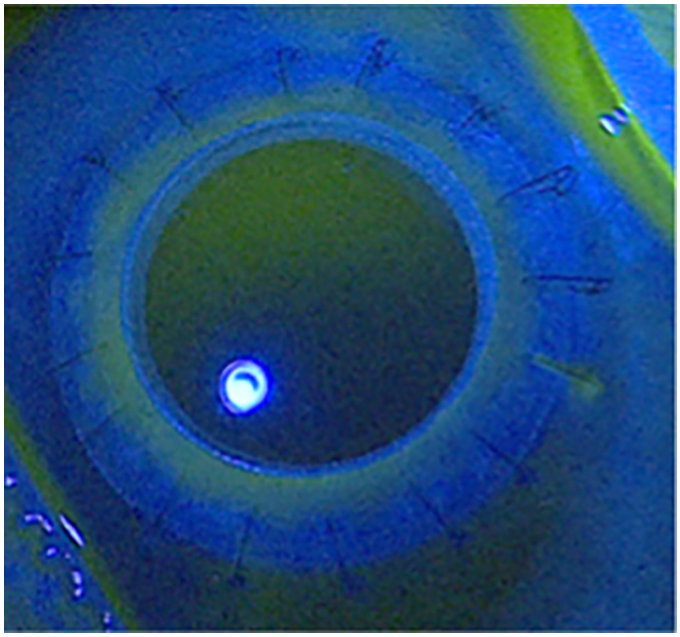

Figure 3. Appearance of the tear film overlying the synthetic corneal device optic stained with fluorescein drops, under cobalt blue illumination.

of the fluorescein dye and the appearance of the first randomly distributed dry spot measured in seconds.

Feasibility of Topical Treatment After Surgery

Both eyes of a single rabbit were used to assess the penetrance of topically applied therapeutics into the anterior chamber 3 months after synthetic corneal device (rabbit version) implantation in the right eye. The experiment was performed under general anesthesia. A single drop of topical latanoprost 0.005% (Alcon Laboratories Inc., Fort Worth, TX) was instilled simultaneously in both eyes. Aqueous humor (100 µL) was sampled from each eye 2 hours after instillation using a 30G needle and submitted for analysis in a masked fashion. The concentration of the latanoprost free acid, which is the active form of the drug in the aqueous humor, was measured using high-pressure liquid chromatography.

Results

Elasticity and Stiffness

The optic stem and skirt material were measured to exhibit a Young's modulus of approximately 6 MPa. The bending stiffness for the thickest section of the skirt at the optic-skirt junction (240 microns) using 1 mm as the plate width was calculated to be 6.9 kPa·mm^4. The stiffness was reduced to 2.5 kPa·mm^4 at the thinnest section, at the skirt edge (170 microns). Figure 4 demonstrates the easy bendability of the skirt at the thickest optic-skirt junction.

Figure 4. The bendability of the skirt with surgical forceps manipulation.

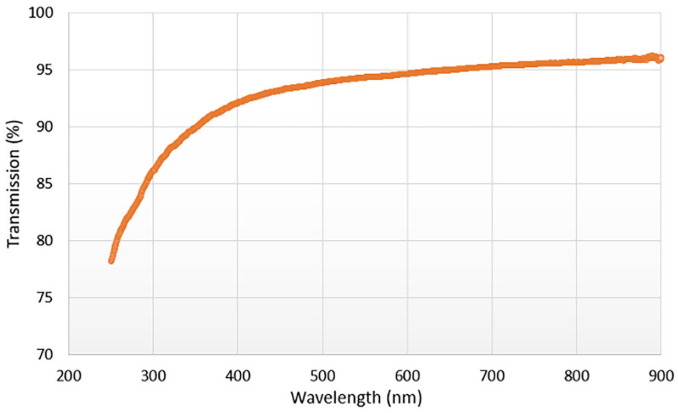

Figure 5. Transmission spectrum of light through the optic of the synthetic corneal device in air.

The biomechanical properties of the human cornea change with age. Nonenzymatic cross-linking, collagen glycation, and an increase in fibril diameter and number of collagen molecules increase with age (>40 years) and cause progressive stiffness. Elastic properties of ex vivo human corneas of various age groups have previously been studied[25] and show a Young's modulus ranging between 0.27 and 0.76 MPa for ages ranging from 20 to 100 years.[25,26] One study measured the in vivo Young's modulus using high-speed Scheimpflug imaging[27] and found the modulus to be approximately 0.205 MPa throughout various age groups (0–64 years).

For the purpose of comparing the bending properties of the fluoroelastic material with the human cornea, a Young's modulus of 0.4 MPa was used as the average human cornea modulus. The bending stiffness for a 1-mm-wide region of 550 µ m average thickness then equals to 5.6 kPa·mm^4. This result shows that the skirt region of the synthetic cornea device with an average modulus of 4.7 kPa·mm^4 is closely aligned with the mechanical properties of the native human cornea.

Light Transmission of the Optic

Light transmission within the visible spectrum[30] ranged between 91% at the shortest wavelength of 380 nm and 96% at the longest wavelength of 780 nm (Fig. 5). Ultraviolet transmission at 300 nm was 86.1%, whereas infrared transmission at 900 nm was 96%. The device transmission characteristics are comparable with that of human corneas in the visible infrared spectrum, which display transmission ranges from 74.5% at 400 nm to 98% at 1000 nm.[31] Ultraviolet transmission in human corneas decreases to 50% at 310 nm,[32,33] whereas transmission through the device

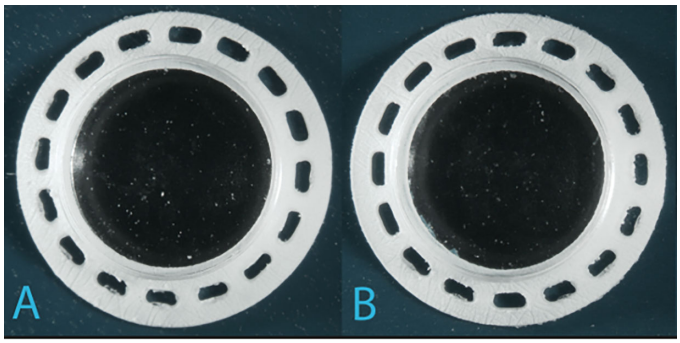

Figure 6. Devices after exposure to prednisolone acetate 1%, without additional cleaning. No visible spoliation was detected after exposure. (A and B) Devices before and after drug exposure, respectively. A high gamma function was applied to enhance any surface deposits.

optic decreases to 86% at 300 nm, which is considerably higher.

Fouling and Wetting

Table details the results of the fouling experiments. Three control devices remained free of staining or debris. Of the 33 experimental devices, none exhibited staining to the optic stem or any sings of degradation.

Thirty of the 33 experimental devices showed no evidence of debris on the optic surface. Among the three devices exposed to prednisolone acetate 1% drops, two displayed superficial, white, crystalline-like deposits on the optic surface. Additionally, one of the three devices that had been exposed to latanoprost showed a single white, crystalline deposit, albeit fully confined within a manufacturing flaw on the optic surface. All surface deposits were eliminated successfully using mechanical means using nonshedding ocular surgical spears made of cellulose.

To determine whether the surface deposits were an experimental artifact, we repeated the spoliation experiment of exposure to prednisolone acetate 1% drops with three additional devices, following the same protocol as described elsewhere in this article. The results showed that all three samples had no deposits, confirming that the deposits in the previous experiment were likely an artifact. The images of a representative device in this repeated test is pictured in Figure 6.

Feasibility of Topical Treatment After Surgery

A small difference was observed in the aqueous humor level of latanoprost in the device eye (62.6 ng/mL) compared with the naïve eye (78.4 ng/mL). This result should be viewed in light of the surface area taken up by the synthetic device within the recipient cornea. Using a spherical cap calculation for the cornea of an average diameter of 11.71 mm and radius of curvature to be 7.79 mm,[34] the surface area of an average human cornea is approximately 130 mm^2. The solid area of the device, occluding the native cornea, is calculated to be approximately 35 mm^2. This area is roughly the same in the rabbit and human versions of the device. The calculation considers the solid optic and the skirt in a spherical cap calculation minus the total surface area of the macro apertures along the skirt. The ratio of occlusion owing to rabbit device (35 mm^2) to the total rabbit corneal surface area (184 mm^2) is approximately 19%. This finding agrees well with the 20% decrease in latanoprost levels in the aqueous humor obtained from the device implanted in the rabbit eye. Similarly, we can calculate the anticipated decrease of surface area for drug penetration in human eye, using the ratio of the occlusion owing to human device (35 mm^2) to the total human corneal surface area (130 mm^2), which is approximately 27%. Nonetheless, during the rabbit experiments,[23,24] no difficulty was noted with regard to pharmacological pupil dilation for fundoscopic examination. This finding suggests that the decrease is likely not clinically significant.

Discussion

The design considerations of our novel synthetic cornea device aimed to address the intrinsic limitations of currently available artificial corneas. In addition to optical clarity, the ideal artificial cornea should exhibit three characteristics: flexibility, biointegration, and epithelialization.[35] We emphasize the clinical relevance of each of these characteristics.

Strong adhesion of the recipient keratocytes along the device, or bioadherence, enables permanent anchorage of the device and minimizes periprosthetic space that is a potential entryway for debris or micro-organisms, even in the absence of epithelial defects. We have previously demonstrated the colonization of the porous expanded polytetrafluoroethylene ingrowth surface by the recipient keratocytes with new collagen deposition along the skirt and optical wall.[23]

Flexibility of the device is crucial to ensure compliance with the recipient native human cornea to minimize the translation of motion of the device at the device–host joint. Otherwise, the perpetual flexural micro-oscillation of the device within the corneal stroma with every blink may trigger inflammation, leading to sterile keratolysis, retroprosthetic

membrane, iris synechiae, and glaucoma. Our device exhibits a bending stiffness that is compatible with the native human cornea. The compliance of the device in conjunction with bioadherence should dampen the shearing forces at the host–device joint.

The light transmission characteristics of the device are comparable to human corneas in the visible infrared spectrum.[31,33] Excellent light transmission is crucial in preserving postoperative visual acuity and color vision. The device exhibits approximately 96% light transmission at infrared wavelengths of 800 to 900 nm, comparable with the 98% transmission of human cornea and allows for compatibility with standard optical coherence tomography imaging, typically utilizing wavelengths of 850 nm.[36] Previous studies have confirmed the feasibility of optical coherence tomography imaging of the anterior segment, optic nerve, and retinal nerve fiber layer for the monitoring of the posterior segment.[23] Although the device exhibits higher UV transmission compared with the human cornea, the native human crystalline lens[37] or lens implant after cataract removal[38] continues to provide the most significant portion of the UV protection for the posterior segment, with UV transmittance falling below 10% through implantable lenses.[38] Therefore, the device is appropriate for pseudophakic human eyes.

Our fouling experiments revealed preservation of optic integrity and clarity in all experimental devices after incubation with commonly used ophthalmic topical medications. All three devices with surface deposits were easily cleared using an ocular surgical spear, suggesting that debris is confined to the surface of the optic. A repeat experiment for three devices with the same drug and protocol yielded a deposit-free device surface, showing that the previously observed debris was likely related to experimental factors. Further testing to assess the impact of a wider range of drugs over a longer incubation time is warranted.

The feasibility of postoperative topical pharmacological treatment is an important requirement for an artificial cornea to help manage infection, inflammation, or glaucoma.[39] There was a small decrease in the aqueous humor level of latanoprost in the device eye compared with the naïve rabbit eye, attributable to the decrease in the surface area of the host cornea taken up by the device. The result is translatable to human eye implanted with a human device with an approximate difference of an 8% increase in the occluded surface area. Further, there were no issues with pharmacological pupil dilation in the rabbit eyes implanted with the device, suggesting that this decrease is not likely to be significant clinically.

The current device prototype does not allow epithelization. Further studies will be directed to achieve this goal to create a device that truly mimics donor cornea.

The Boston type 1 keratoprosthesis is the most widely implanted artificial cornea worldwide.[40] It is largely indicated as an alternative in cases of previous graft failure or as a primary intervention in patients at high risk of donor graft failure.[41] Although the device is able to restore significant functional vision in many patients with severe corneal disease, patients must be monitored closely postoperatively owing to risks for retroprosthetic membrane formation, glaucoma, infection, and extrusion, particularly with longer follow-up.[41] Thus, the use of the device has decrease steadily worldwide.[16,17] The intrinsic limitation of the device design that cannot be overcome is its rigidity. The optic is made of polymethylmethacrylate, with a back plate made from polymethylmethacrylate or titanium. These materials are biologically inert but compact, and they do not allow for tissue ingrowth. As mentioned elsewhere in this article, the lack of adherence at the optic wall results in repeated oscillatory shear force at the host–device joint generated from each blink, which translates to kinetic energy absorbed by the surrounding corneal stroma causing inflammation, tissue wear, and thinning.[42,43] In addition, the periprosthetic potential space owing to lack of adhesion is a risk factor for infection.

The current global unmet need for access to corneal transplantation cannot be solved through increasing the supply of donor corneas alone. More than one-half (53%) of the world's population does not have access to eye banking systems.[4] The majority of corneal blindness exists in areas without proper infrastructure to support eye banking, including an inability to maintain a cold chain for tissue transport, limited storage facilities and appropriately trained personnel, and inadequate donor retrieval capabilities.[44] Using a fully synthetic artificial cornea in place of traditional keratoplasty in resource-limited areas may be a solution to overcome costly eye banking issues. This solution is constrained currently by financial limitations, because countries where artificial corneal transplants could provide significant benefit to corneally blind largely lack the financial means to support widespread access to artificial corneas. Hence, the research to create an ideal and cost-effective artificial cornea continues.

In conclusion, this novel, fully synthetic device may be an alternative in areas of the world without access to corneal transplantation or in developed nations for patients with a history of repeat keratoplasty failure. An early feasibility study in human patients is currently underway.

Acknowledgments

The authors thank Harrison Norman, W.L. Gore & Associates, for assistance with the fouling experiments.

Johns Hopkins University, Esen K. Akpek's employer, has received an institutional research grant from W.L. Gore & Associates Inc. related to this project.

Disclosure: **G. Li**, None; **A.J. Aldave**, W.L. Gore & Associates Inc. (C); **G. Amescua**, W.L. Gore & Associates Inc. (C); **K.A. Colby**, W.L. Gore & Associates Inc. (C); **M.S. Cortina**, W.L. Gore & Associates Inc. (C); **J. de la Cruz**, W.L. Gore & Associates Inc. (C); **J.-M.A. Parel**, W.L. Gore & Associates Inc. (C); **T.B. Schmiedel**, W.L. Gore & Associates Inc. (E); **E.K. Akpek**, W.L. Gore & Associates Inc. (C)

References

1. Vashist P, Senjam SS, Gupta V, et al. Blindness and visual impairment and their causes in India: results of a nationally representative survey. *PLoS One*. 2022;17(7):e0271736, doi:10.1371/journal.pone.0271736.
2. Tran TM, Duong H, Bonnet C, Kashanchi A, Buckshey A, Aldave AJ. Corneal blindness in Asia: a systematic review and meta-analysis to identify challenges and opportunities. *Cornea*. 2020;39(9):1196–1205, doi:10.1097/ICO.0000000000002374.
3. Maghsoudlou P, Sood G, Akhondi H. Cornea transplantation. In: *StatPearls*. St. Petersburg, FL: StatPearls Publishing; 2022. Accessed December 5, 2022, http://www.ncbi.nlm.nih.gov/books/NBK539690/.
4. Gain P, Jullienne R, He Z, et al. Global survey of corneal transplantation and eye banking. *JAMA Ophthalmol*. 2016;134(2):167–173, doi:10.1001/jamaophthalmol.2015.4776.
5. Alio JL, Montesel A, El Sayyad F, Barraquer RI, Arnalich-Montiel F, Alio Del Barrio JL. Corneal graft failure: an update. *Br J Ophthalmol*. 2021;105(8):1049–1058, doi:10.1136/bjophthalmol-2020-316705.
6. Eye Bank Association of America. 2021 Eye Banking Statistical Report. Published online April 2022.
7. Eye Bank Association of America. 2001 Eye Banking Statistical Report. Published online March 2002.
8. Bigan G, Puyraveau M, Saleh M, et al. Corneal transplantation trends in France from 2004 to 2015: a 12-year review. *Eur J Ophthalmol*. 2018;28(5):535–540, doi:10.1177/1120672118762224.
9. Flockerzi E, Maier P, Böhringer D, et al. Trends in corneal transplantation from 2001 to 2016 in Germany: a report of the DOG-Section Cornea and its Keratoplasty Registry. *Am J Ophthalmol*. 2018;188:91–98, doi:10.1016/j.ajo.2018.01.018.
10. Chan SWS, Yucel Y, Gupta N. New trends in corneal transplants at the University of Toronto. *Can J Ophthalmol*. 2018;53(6):580–587, doi:10.1016/j.jcjo.2018.02.023.
11. Aboshiha J, Jones MNA, Hopkinson CL, Larkin DFP. Differential survival of penetrating and lamellar transplants in management of failed corneal grafts. *JAMA Ophthalmol*. 2018;136(8):859–865, doi:10.1001/jamaophthalmol.2018.1515.
12. Fukuoka S, Honda N, Ono K, Mimura T, Usui T, Amano S. Extended long-term results of penetrating keratoplasty for keratoconus. *Cornea*. 2010;29(5):528–530, doi:10.1097/ICO.0b013e3181c29705.
13. Ahmad S, Mathews PM, Lindsley K, et al. Boston type 1 keratoprosthesis versus repeat donor keratoplasty for corneal graft failure: a systematic review and meta-analysis. *Ophthalmology*. 2016;123(1):165–177, doi:10.1016/j.ophtha.2015.09.028.
14. Bonneau S, Tong CM, Yang Y, Harissi-Dagher M. The treatment of end-stage corneal disease: penetrating keratoplasty compared with Boston type 1 keratoprosthesis. *Graefes Arch Clin Exp Ophthalmol*. 2022;260(9):2781–2790, doi:10.1007/s00417-022-05646-1.
15. Akpek EK, Cassard SD, Dunlap K, Hahn S, Ramulu PY. Donor corneal transplantation vs Boston type 1 keratoprosthesis in patients with previous graft failures: a retrospective single center study (an American Ophthalmological Society thesis). *Trans Am Ophthalmol Soc*. 2015;113:T3.
16. Lee WB, Shtein RM, Kaufman SC, Deng SX, Rosenblatt MI. Boston keratoprosthesis: outcomes and complications: a report by the American Academy of Ophthalmology. *Ophthalmology*. 2015;122(7):1504–1511, doi:10.1016/j.ophtha.2015.03.025.
17. Chodosh J, Gelfand L, Paschalis E. Boston Kpro news Issue XVI (2021). Published online October 2021, https://www.masseyeandear.org/assets/MEE/pdfs/professionals/kpro/2021kpronewsletter.pdf.

18. Aravena C, Yu F, Aldave AJ. Long-term visual outcomes, complications, and retention of the Boston type I keratoprosthesis. *Cornea*. 2018;37(1):3, doi:10.1097/ICO.0000000000001405.
19. Aoun T, Harissi-Dagher M. Long-term visual outcomes of Boston type I keratoprosthesis in Canada. *J Fr Ophtalmol*. 2023;46(10):1212–1221, doi:10.1016/j.jfo.2023.07.014.
20. Wang LQ, Wu TY, Chen XN, et al. Long-term outcomes of Boston keratoprosthesis type I: the Chinese People's Liberation Army General Hospital experience. *Br J Ophthalmol*. 2022;106(6):781–785, doi:10.1136/bjophthalmol-2019-315617.
21. Kim MJ, Bakhtiari P, Aldave AJ. The international use of the Boston type I keratoprosthesis. *Int Ophthalmol Clin*. 2013;53(2):79–89, doi:10.1097/IIO.0b013e31827ab3d3.
22. Pineda R. Corneal transplantation in the developing world: lessons learned and meeting the challenge. *Cornea*. 2015;34:S35, doi:10.1097/ICO.0000000000000567.
23. Akpek EK, Aldave AJ, Amescua G, et al. Twelve-month clinical and histopathological performance of a novel synthetic cornea device in rabbit model. *Transl Vis Sci Technol*. 2023;12(8):9, doi:10.1167/tvst.12.8.9.
24. Akpek EK, Van Court S, Glass S, Schmiedel T, Troutman M. Short-term clinical outcomes of a novel corneal prosthetic device in a rabbit model. *Cornea*. 2020;39(6):706–712, doi:10.1097/ICO.0000000000002266.
25. Lam AKC, Hon Y, Leung LKK, Lam DCC. Repeatability of a novel corneal indentation device for corneal biomechanical measurement. *Ophthalmic Physiol Opt*. 2015;35(4):455–461, doi:10.1111/opo.12219.
26. Knox Cartwright NE, Tyrer JR, Marshall J. Age-related differences in the elasticity of the human cornea. *Invest Ophthalmol Vis Sci*. 2011;52(7):4324–4329, doi:10.1167/iovs.09-4798.
27. Shih PJ, Huang CJ, Huang TH, et al. Estimation of the corneal Young's modulus in vivo based on a fluid-filled spherical-shell model with Scheimpflug imaging. *J Ophthalmol*. 2017;2017:5410143, doi:10.1155/2017/5410143.
28. Efron N, Young G, Brennan NA. Ocular surface temperature. *Curr Eye Res*. 1989;8(9):901–906.
29. Chirila TV, Morrison DA, Hicks CR, Gridneva Z, Barry CJ, Vijayasekaran S. In vitro drug-induced spoliation of a keratoprosthetic hydrogel. *Cornea*. 2004;23(6):620–629, doi:10.1097/01.ico.0000121703.74077.ea.
30. Sliney DH. What is light? The visible spectrum and beyond. *Eye*. 2016;30(2):222–229, doi:10.1038/eye.2015.252.
31. Beems EM, Van Best JA. Light transmission of the cornea in whole human eyes. *Exp Eye Res*. 1990;50(4):393–395, doi:10.1016/0014-4835(90)90140-P.
32. Boettner EA, Wolter JR. Transmission of the ocular media. *Invest Ophthalmol Vis Sci*. 1962;1(6):776–783.
33. Doutch JJ, Quantock AJ, Joyce NC, Meek KM. Ultraviolet light transmission through the human corneal stroma is reduced in the periphery. *Biophys J*. 2012;102(6):1258–1264, doi:10.1016/j.bpj.2012.02.023.
34. Rüfer F, Schröder A, Erb C. White-to-white corneal diameter: normal values in healthy humans obtained with the Orbscan II topography system. *Cornea*. 2005;24(3):259–261, doi:10.1097/01.ico.0000148312.01805.53.
35. Hicks CR, Fitton JH, Chirila TV, Crawford GJ, Constable IJ. Keratoprostheses: advancing toward a true artificial cornea. *Surv Ophthalmol*. 1997;42(2):175–189, doi:10.1016/s0039-6257(97)00024-6.
36. Ruggeri M, Wehbe H, Jiao S, et al. In vivo three-dimensional high-resolution imaging of rodent retina with spectral-domain optical coherence tomography. *Invest Ophthalmol Vis Sci*. 2007;48(4):1808–1814, doi:10.1167/iovs.06-0815.
37. Fukuoka H, Gali HE, Bu JJ, Sella R, Afshari NA. Ultraviolet light exposure and its penetrance through the eye in a porcine model. *Int J Ophthalmol*. 2023;16(2):172–177, doi:10.18240/ijo.2023.02.02.
38. Mainster MA. The spectra, classification, and rationale of ultraviolet-protective intraocular lenses. *Am J Ophthalmol*. 1986;102(6):727–732, doi:10.1016/0002-9394(86)90400-9.
39. Holland G, Pandit A, Sánchez-Abella L, et al. Artificial cornea: past, current, and future directions. *Front Med*. 2021;8:770780, doi:10.3389/fmed.2021.770780.
40. Dohlman C. The Boston keratoprosthesis-the first 50 years: some reminiscences. *Annu Rev Vis Sci*. 2022;8:1–32, doi:10.1146/annurev-vision-100820-021253.
41. Milad D, Yang Y, Eisa K, Harissi-Dagher M. Review of clinical trials addressing the Boston Keratoprosthesis. *Can J Ophthalmol*. 2023 May 27:S0008-4182(23)00166-7. Published online May 27, 2023, doi:10.1016/j.jcjo.2023.05.003.

42. Grassi CM, Cruzat A, Taniguchi EV, et al. Periprosthetic tissue loss in patients with idiopathic vitreous inflammation after the Boston keratoprosthesis. *Cornea*. 2015;34(11):1378–1382, doi:10.1097/ICO.0000000000000557.
43. Dudenhoefer EJ, Nouri M, Gipson IK, et al. Histopathology of explanted collar button keratoprostheses: a clinicopathologic correlation. *Cornea*. 2003;22(5):424–428, doi:10.1097/00003226-200307000-00007.
44. Gupta N, Vashist P, Ganger A, Tandon R, Gupta SK. Eye donation and eye banking in India. *Natl Med J India*. 2018;31(5):283–286, doi:10.4103/0970-258X.261189.